

Association Behaviors of  
Poly(*N*-vinylpyrrolidone)-Grafted Fullerenes in Aqueous Solution

Emiko Mouri\*, Sanami Moroi,

Department of Applied Chemistry, Faculty of Engineering, Kyushu Institute of Technology, 1-1 Sensui,  
Tobata, Kitakyushu, Fukuoka 804-8550, Japan

\*To whom correspondence should be addressed.

e-mail: mouri@che.kyutech.ac.jp, Tel & Fax: +81-93-884-3335

ORCID iD (Dr. Emiko Mouri) [0000-0002-0148-0371](https://orcid.org/0000-0002-0148-0371)

Short Title: PVP-Grafted Fullerenes in Aqueous Solution

Key words: poly(*N*-vinylpyrrolidone); fullerene; micelle; assembly; polymer

## **Abstract**

Poly(*N*-vinylpyrrolidone) (PVP)-grafted fullerenes (PVP-C<sub>60</sub> and PVP-C<sub>70</sub>) were synthesized by iniferter polymerization in order to fabricate water-soluble fullerene containing micelles. PVP-C<sub>60</sub> formed micelles with hydrodynamic diameters ranging from 15 nm to 33 nm. The solubilization of fullerene molecules into the core of the PVP-C<sub>60</sub> micelles was also found to control the size of the micelles. By increasing the amount of added fullerene, we gradually increased the micelle size before drastically increasing it to that of 200 nm in hydrodynamic diameter. The drastic change occurred at a critical value of the added C<sub>60</sub>/PVP monomer ratio, almost independently of the molecular weight of PVP.

## **Introduction**

Fullerene (C<sub>60</sub>) is one of the most attractive materials in nanomaterial science because of its specific shape and versatile characteristics such as semiconductivity, high thermal stability, radical-trapping properties, and high refractive index [1,2]. Fullerene has been reported to be effective for medical and cosmetic purposes [3-7]. For example, it is a promising candidate for use in medicine in the treatment of cancer and HIV infection [3,6]. One important issue in the application of fullerene that must be overcome is its low solubility in solvents; in applications such as drug delivery, particularly, fullerenes must be dispersed in aqueous solution. To achieve this, fullerenes are usually modified by the introduction of polar groups or hydrophilic polymers [8,9]. In order to establish *in vivo* applications using fullerenes, it

is imperative to ascertain the size effect of fullerene-containing materials on the human body and the solubility of this material in water. In particular, the size effect on drug effectiveness and toxicity cannot be ignored in the range extending from a few nanometers to 100 nm. In order to assess the size effect of this material, we fabricated a well-characterized fullerene-containing micelle system in water.

From the late 1990s to the present, many types of polymer-grafted fullerenes with a relatively monodisperse nature have been synthesized [2,9], such as some very sophisticated systems [10]. In some cases, however, the diameter of these assemblies exceeds 100 nm, which is enormously large for a micellar system [11-13]. We also reported recently that poly(methyl methacrylate)-grafted fullerene forms a monodisperse assembly with a sub-micrometer diameter [14]. Also in this case, the large assembly is suggested to possess a hierarchical structure and form from micelles as building blocks. On the other hand, micelles of about 3–5 nm hydrodynamic radius were observed in systems containing poly[2-(dimethylamino)-ethyl methacrylate] [15]. The observed large aggregation was attributed to a strong adhesion force between  $C_{60}$ ; thus, designing a polymer structure with the ability to overcome this adhesion force is necessary. Okamura et al. synthesized disubstituted fullerenes by attaching two polymer chains from two neighboring sites to a single fullerene molecule [16]. They confirmed that the micelle size is 40 nm in the radius of gyration [17]. Inspired by these studies, we attempted to synthesize poly(*N*-vinylpyrrolidone) (PVP)-grafted fullerenes to form micelles with < 20 nm diameter in aqueous solution. We expected the micelles to form rather than large aggregates because of the presence of the

bulky pyrrolidone groups. PVP is also non-toxic, water-soluble that is widely used as a dispersant in the medical and cosmetic industries. Nevertheless, the association behavior of PVP-grafted fullerene has been scarcely reported upon.

Among the PVP–fullerene systems, the PVP/C<sub>60</sub> and PVP/C<sub>70</sub> complex systems have been mainly studied [18-22]. In these systems, fullerene and PVP are not covalently bonded, and the complexes of PVP and fullerene formed via donor–acceptor interaction [20]. Advantages of the complex system are intact fullerene and retention of the biological activity of fullerene. However, the size control of these PVP/fullerene complexes is difficult because the complex formation is sensitive to the surrounding conditions, i.e., the concentration, ionic strength, and pH. In recent years, Yamakoshi et al. reported upon the synthesis of covalently bonded PVP–fullerene systems [23,24]. By utilizing RAFT polymerization, they succeeded in obtaining PVP-grafted fullerene with a relatively narrow polydispersity. However, the reported assembly size of PVP-C<sub>60</sub> is very large (up to 560 nm) in comparison with the usual micelle size, and the molecular weight or some parameters of this system would be a key factor controlling the assembly size.

In this paper, we report the synthesis of PVP-grafted fullerenes (PVP-C<sub>60</sub> and PVP-C<sub>70</sub>) in aqueous solution utilizing a photoiniferter [25]. The elucidated characteristics of this system were determined using dynamic light scattering. We found that PVP-grafted fullerenes form micelles with 15 to 30 nm hydrodynamic diameter in aqueous solution. We demonstrated that the fabricated micelles are not

sensitive to ethanol and added salt, a crucial characteristic for in vivo treatment. The solubilization characteristics of PVP-C<sub>60</sub> were estimated by adding free fullerenes. A gradual increase in micelle size was observed upon the addition of free fullerenes with diameter up to ca. 30 nm; however, a drastic increase in size indicating the formation of monodisperse assemblies 200 nm in size was also observed.

## Experimental Section

### Synthesis of PVP-Grafted Fullerene

First, a photoiniferter reagent, benzyl *N, N*-dithiocarbamate (BDDC), was synthesized: 5 g of sodium *N, N*-diethyldithiocarbamate (Wako Pure Chemical Industries, Ltd, Osaka, Japan) was stirred in ethanol for 30 min with ice. Then, 1.7 ml of benzyl chloride (Wako Pure Chemical Industries, Ltd, Osaka, Japan) mixed with 5 ml of ethanol was added to the reaction, which was stirred for 5 h at room temperature. The crude product was filtered, and the filtrate was extracted with a mixture of water and ether. The ether fraction was dried with MgSO<sub>4</sub>, filtered, and dried in by rotary evaporation to obtain BDDC with 60% of yield (Supporting Information Figure S1).

In the next step, PVP was synthesized by photoiniferter polymerization, through initiation using BDDC, as shown in **Scheme 1**. *N*-Vinylpyrrolidone (Wako Pure Chemical Industries, Ltd, Osaka, Japan), BDDC, and ethanol in a test tube were degassed through several freeze/thaw cycles to remove oxygen, followed by the sealing of the test tube under reduced pressure and 4–5 h of UV irradiation using

high-pressure mercury lamps (SX-UI500HQ and BA-H500; USIO Inc., Tokyo, Japan). The feeds and irradiation conditions for each sample are summarized in supporting information (Table S1). After irradiation, PVP was obtained through re-precipitation with diethyl ether. The molecular weights were estimated using  $^1\text{H}$  NMR spectroscopy (Avance-400; Bruker, Illinois, USA) and GPC, as shown in **Table 1** (Supporting Information Figure S2). The GPC system was equipped with a column oven (CTO-10A/10AC; Shimadzu, Kyoto, Japan) and a refractive index detector (RI153; Jasco Corp., Tokyo, Japan). *N,N*-Dimethylformamide was used as an eluent, and polyethylene glycol (PEG) and polystyrene (PSt) were used as standards. We could not determine number-averaged molecular weight  $M_n$  using  $^1\text{H}$  NMR spectroscopy for samples with large molecular weights because the peak representing the phenyl group at the end of the PVP chain was too weak.

In the third step, fullerene was grafted using the as-synthesized PVP. The feeding molar ratio of PVP to fullerene is adjusted to be 1:3 not to obtain fullerenes grafted with plural PVP chains. In the reaction, PVP, fullerene (Fullerene, nanom purple st 98%, Frontier carbon, Fukuoka, Japan), and 1-hydroxycyclohexylphenyl ketone (Wako Pure Chemical Industries, Ltd, Osaka, Japan) were mixed in dichlorobenzene under a nitrogen atmosphere and irradiated with UV light for 8-12 h depending on the sample to obtain fullerene capped PVP (**Scheme 2**). Representative feeds for samples are summarized in Table S2. We carried out the reaction several times for the same PVP samples to obtain a reasonable amount of samples. The C–S bond in PVP can be broken to form two radicals during the iniferter

polymerization (**Scheme 1**), which then react with fullerene in this step. The radical-trapping nature of fullerene makes the reaction smoother.

The crude product was shaken several times with water and toluene to remove any free fullerene. The water fraction was extracted and evaporated, and then the residue was re-dissolved in ethanol to further remove the free fullerene via centrifugal separation. In order to remove free PVP, dialysis against water was carried out. The dialysis was continued until the UV spectrum of the sample was unchanged (Supporting Information Figure S3). Through this procedure, free fullerene and free PVP were removed from the stock sample.

The presence of PVP-C<sub>60</sub> was confirmed by <sup>13</sup>C NMR spectroscopy (JNM-A500; JEOL, Tokyo, Japan; Supporting Information Figures S4, S5). <sup>13</sup>C NMR spectroscopy was carried out with solid samples. TGA measurements were also carried out in order to estimate the PVP:C<sub>60</sub> ratio (Supporting Information Figure S6). The C<sub>60</sub> weight fraction at 600 °C was estimated because 99% of the PVP was burned off at 600 °C. In the same manner, PVP-grafted C<sub>70</sub> was also prepared.

### **Size Estimation of Self-Assemblies**

The surface tension was measured using a CBVP-A3 tensiometer (Kyowa, Tokyo, Japan). Measurement was done through the Wilhelmy method, in which a platinum plate is placed on the surface of the sample solution and the force on the plate is measured at 25°C. Above the critical micelle concentration (CMC), dynamic light scattering (DLS-7000; Otsuka Electronics Co, Ltd., Osaka, Japan)

was performed using a He–Ne laser ( $\lambda=632.8$  nm). We obtained the time correlation function,  $g^2(\tau)$ , of the measured scattered intensity defined by the following equation:

$$g^2(t) = \frac{\langle I(t) I(t + t) \rangle}{\langle I(t) \rangle^2},$$

where  $I(t)$  is the scattered intensity at time  $t$ , and  $\tau$  is the delay time. The time-correlation of the scattering intensities is calculated at every delay time  $\tau$ . Delay time  $\tau$  is the time difference between the arbitrary two correlated data points. The time correlation function of scattered amplitude,  $g^1(\tau)$ , is related to  $g^2(\tau)$  by the following equation;

$$g^2(\tau) - 1 = \beta |g^1(\tau)|^2,$$

where  $\beta$  is the coherent factor. Data analysis was carried out by the curve fitting of  $(g^2-1)^{1/2}$  to exponential function  $\beta^{1/2} \exp(-\Gamma\tau)$  as  $g^1(\tau) = \exp(-\Gamma\tau)$ . In the fitting, decay rate  $\Gamma$  and coherent factor  $\beta$  are the fitting parameters. When the single exponential model cannot reproduce the data, we introduce a double exponential model as  $(g^2-1)^{1/2} = \phi(\beta^{1/2} \exp(-\Gamma_1\tau)) + (1-\phi)(\beta^{1/2} \exp(-\Gamma_2\tau))$  with  $\phi$  as a fraction of the first component. Maquardt analysis was also performed in addition to exponential fitting.

Almost all of the data could be fitted well with a double exponential function. By changing the scattering angle from  $75^\circ$  to  $120^\circ$ , a plot of decay rate ( $\Gamma$ ) vs. scattering vector ( $q^2$ ) was constructed. The scattering vector is defined as  $q = 4\pi n \sin \theta / \lambda$ , where  $n$  is a refractive index,  $\theta$  is scattering angle, and  $\lambda$  is laser wavelength. Using the linear relationship, we confirmed the observation of a lateral diffusion mode. The established relationship  $\Gamma = Dq^2$ , where  $D$  is the diffusion coefficient determined from the slope of

the plot, was used to find the hydrodynamic diameter of the system using the Stokes–Einstein equation ( $D_h = kT/3\pi\eta D$ , where  $D_h$  is the hydrodynamic diameter,  $k$  is the Boltzmann's constant,  $T$  is absolute temperature,  $\eta$  is the solvent viscosity, and  $D$  is the diffusion coefficient). DLS measurements were carried out for mixed system of free PVP and  $C_{60}$  for comparison with the PVP- $C_{60}$  systems. Furthermore, dried PVP- $C_{60}$  micelles were observed directly by TEM using an H-7650.

### **Solubilization of $C_{60}$ into PVP- $C_{60}$ Micelles**

PVP- $C_{60}$  was dissolved in chloroform (0.6~0.8 gL<sup>-1</sup>) and mixed with a toluene solution of  $C_{60}$  (0.01 gL<sup>-1</sup>). For example, the amount of toluene solution (0.01 gL<sup>-1</sup>) was varied from ca. 0.2 to 10 ml against 2ml of chloroform solution in PVP3k- $C_{60}$  system. The experimental conditions for other samples are summarized in Table S6. After evaporation, the residue was re-dispersed in water. Redispersion in water and evaporation was repeated three times to remove chloroform and toluene completely. With the obtained dispersion, the micelle size with solubilized  $C_{60}$  was estimated by DLS. This procedure was executed for each sample with different amounts of  $C_{60}$ . PVP- $C_{60}$  micelles with solubilized  $C_{60}$  at dried state were observed by TEM using an H-9000NAR (Hitachi, Tokyo, Japan)

## **Results and Discussion**

Synthesis of PVP- $C_{60}$  was carried out by the process shown in **Schemes 1** and **2**. The obtained PVP samples were characterized by <sup>1</sup>H NMR spectroscopy and GPC [<sup>1</sup>H NMR (D<sub>2</sub>O) for PVP:  $\delta$ : 1.28 (m,

N(CH<sub>2</sub>CH<sub>3</sub>)<sub>2</sub>), 3.25 (m, N-CH<sub>2</sub>), 7.2–7.5 (m, Ph) ppm; Supporting Information Figure S1]. Characteristics of the PVP-C<sub>60</sub> samples containing PVP with different molecular weights are given in **Table 1**. The molecular weights estimated by <sup>1</sup>H NMR spectroscopy are absolute values, while those estimated from GPC are relative values. In particular, the averaged molecular weights estimated by <sup>1</sup>H NMR spectroscopy and GPC for two different standard polymers (PEG and PSt) are vastly different, as shown in **Table 1**. We named the samples as PVPXk-C<sub>60</sub> mainly based on the number-averaged molecular weight obtained from <sup>1</sup>H NMR.

The confirmation of C<sub>60</sub> present in the samples was performed by <sup>13</sup>C NMR spectroscopy (Supporting Information Figure S5) and UV spectrum analysis (**Figure 1**). In the <sup>13</sup>C NMR spectrum (Figure S5), the peak around 135–160 ppm corresponds to fullerene aromatic carbons, which is not confirmed in <sup>13</sup>C NMR of PVP (Figure S4). In addition to that, the UV–vis spectra of the PVP and PVP-C<sub>60</sub> samples were also compared, as shown in **Figure 1**. We can confirm from the PVP-C<sub>60</sub> spectrum strong absorptions at around 260 and 330 nm, which are attributed to the grafting of C<sub>60</sub> to PVP [24]. Free fullerene mixed with a PVP homopolymer in water showed absorption at 240, 275, and 345 nm (data not shown). The wavelength shift suggests the formation of a chemical bond between the C<sub>60</sub> and PVP components.

We also estimated the fullerene-to-PVP ratio. In the TGA measurements, PVP:C<sub>60</sub> values based on molecular weight (obtained by GPC using PEG standards) ranged from 1:1 to 1:4.5 depending on the

samples as shown in Table S3. This finding suggests that plural fullerene molecules may attach to one PVP chain. However, clear shifts of peak position between PVP and C<sub>60</sub>-attached PVP were not confirmed by the GPC measurements (Supporting Information Figure S7). We concluded that we mainly obtained C<sub>60</sub>-encapped PVP. The polydispersity of PVP would contribute the result.

**Figure 2** shows the surface tension variation with the concentration of sample PVP10k-C<sub>60</sub>. (Sample characteristics are summarized in **Table 1**.) We measured the surface tension of PVP10k-C<sub>60</sub> aqueous solutions at 25 °C. The CMC was confirmed to be around 1 μM (ca. 0.001 wt%). We confirmed that PVP of different molecular weight shows almost same in surface tension measurement in the corresponding range from the reference [26]. In the literature, PVP with molecular weight of 10,000 and 55,000 are compared, which almost cover our studied range. Thus, we assume that the CMC would be similar among the samples we treated.

Upon attachment of the C<sub>60</sub> molecule at the end of the PVP chain, a decrease in surface tension was observed at a lower concentration by two orders of magnitude. Noskov et al. measured the surface tension of a PVP (M<sub>n</sub> = 10,000) solution and reported a drastic decrease in surface tension at around 0.1 wt%, and it takes much time to achieve the equilibrium [26]. A lower CMC value for PVP-C<sub>60</sub> indicates high surface activity; thus, that surface activity is elevated when fullerene is attached to the end of the PVP chain. The surface tension decreased to 65 mN/m in PVP-C<sub>60</sub> relative to that of pure water, as shown in **Figure 2**, indicating that PVP-C<sub>60</sub> was adsorbed at the air/water interface. In addition to that, the shape

of the curvature of (surface tension)-Log(concentration) plot of PVP-C<sub>60</sub> is much different from that of PVP [26]. The shape of the curvature for PVP-C<sub>60</sub> is more like typical amphiphilic molecules, which is reasonable considering the molecular architecture of PVP-C<sub>60</sub>. These characteristics indicates the rather weak surface activity of PVP-C<sub>60</sub> in surface tension decrease but efficiency by small amount, which is a desired characteristic considering the incorporation of PVP-C<sub>60</sub> into living systems.

Above the CMC, DLS measurements were conducted to estimate the size of micelles or any other assembly. **Figure 3** is a representative time correlation function obtained at the scattering angle of 90° by DLS measurement. In order to reconstruct the time-correlation function, a double exponential model was used. By plotting decay rate  $\Gamma$ , at each scattering angle against scattering vector  $q$ , we obtained  $q^2$ - $\Gamma$  plots (**Figure 4**), which show good linearity. In general, the linearity indicates that the samples behave as rigid spheres with a lateral diffusion mode. It is reasonable to say that the micelles of PVP-C<sub>60</sub> are spherical rather than rod- or disc-shaped, although the exact shape of the micelle should be estimated via small-angle X-ray (or neutron) scattering or static light-scattering measurements. The hydrodynamic diameters obtained using the gradient of the  $q^2$ - $\Gamma$  plots are listed in **Table 1** together with their number fractions. The number fraction presented here was obtained from Maquardt analysis. (Representative data from the Maquardt analysis are presented in Table S4, along with the standard deviation in hydrodynamic diameter obtained by the data at a 90° scattering angle.) The majority of the micelles formed in the aqueous solution had hydrodynamic diameters that ranged from 15 to 33 nm. A

small portion of micelles (less than 1% number fraction) formed large assemblies about 140~300 nm in hydrodynamic diameter.

TEM observations of the dried micelles confirmed their averaged diameter to be around 31-35 nm, as shown in **Figure 5** and **Figure S8**. Although the size of dried micelle observed by TEM is rather larger than the hydrodynamic diameter obtained by DLS, it is reasonable result considering the deformation of micelles in a drying process. The large assemblies with diameters of around 200 nm were not observed by TEM, in agreement with the very small fraction of large assemblies as measured by DLS. However, PVP-C<sub>60</sub> assembly size range shown here is much smaller than those reported previously [24]. Yamakoshi et al. reported a large assembly composed of smaller spherical parts [24]. In our case, we might see the smaller spherical parts separately. The difference may be raised by the concentration or minor structural difference of PVP-C<sub>60</sub>.

The micelle size of PVP-C<sub>70</sub> was also estimated in the same manner. **Figure 6** shows the molecular-weight dependence of the micelle sizes for PVP-C<sub>60</sub> and PVP-C<sub>70</sub>. The micelle size ranged from 15 to 33 nm, increasing as the PVP molecular weight increased from 3,000 to 45,000. Furthermore, almost no difference between the C<sub>60</sub> and C<sub>70</sub> systems was observed. In the C<sub>70</sub> system, however, fitting a model to the DLS data was more difficult than it was for the PVP-C<sub>60</sub> system. This difficulty may be attributed to the light adsorption of C<sub>70</sub> around 600 nm, a value close to the He-Ne laser wavelength. Thus, discussions hereafter will be focused on PVP-C<sub>60</sub> aqueous solutions.

The micelle sizes obtained by DLS are reasonable when considering the size of the PVP–fullerene molecule. For example, the maximum size, i.e., the size obtained with a fully extended PVP chain of PVP3k-C<sub>60</sub> molecules, was calculated to be 8 nm. In a spherical micelle, two such molecules are involved; the maximum micelle diameter should therefore be 16 nm. Considering that the hydrodynamic diameters are estimated to be larger than the real diameter, a value of 15 nm for this dimension for PVP3k-C<sub>60</sub> is reasonable. The association number of forming a single micelle was also calculated. In the calculation, the hydrodynamic diameter (15–33 nm) was divided by the volume occupied by a PVP-C<sub>60</sub> molecule. The volume of PVP-C<sub>60</sub> was estimated from the bulk density of PVP and the diameter of C<sub>60</sub>. In this calculation, we did not consider water, which should exist in the PVP shell. The association number ranged from 240 to 390 when PVP:C<sub>60</sub> remained at a 1:1 ratio with assuming PVP bulk density of 1.2 g/cm<sup>3</sup>. Therefore, we can reasonably state here that the association number in this system is around 300 for the present study.

The effects of the addition of salt and the solvent ethanol were investigated to assess the *in vivo* applicability of this system. **Figure 7** shows a  $q^2$ - $\Gamma$  plot for PVP10k-C<sub>60</sub> in a 0.15 M NaCl aqueous solution (i.e., saline). As in the former case, good linearity was confirmed in  $q^2$ - $\Gamma$  plots. The micelle diameter was estimated to be 20 nm, as shown in **Table 2**, which is almost the same as that in water. We confirmed that the PVP-C<sub>60</sub> micelle did not aggregate in saline, as is required for *in vivo* applications. (Representative data from the Maquardt analysis are presented in Table S5, along with the standard

deviation in hydrodynamic diameter obtained by the data at a 90° scattering angle.) In ethanol, the micelle size decreased to a diameter of 12 nm. This may be attributed to a decrease in the micellar association number, which is caused by the diffused state of PVP chains in ethanol. We assessed the solvent quality to PVP, and ethanol is more like good solvent than pure water based on solubility parameters [27]. Solubility parameter values ( $\delta$ ) for water, ethanol, and PVP are 47.9, 20.5 and 25.6 MPa<sup>1/2</sup>, respectively. Polymer-solvent interaction is characterized by  $\chi$  which has linear relationships with  $(\delta_1 - \delta_2)^2$ . Based on this relationships,  $\chi$  in PVP-ethanol system is smaller than that of PVP-water system. Thus, PVP chains can form a more diffused state in ethanol than in water. In such case, PVP chains diffuse and occupy a larger volume than in water. Similar effect of ethanol is also observed in comparable system, poly(methacrylic acid)-grafted fullerene system studied by our group [28].

In order to demonstrate the contrast between these PVP-grafted fullerene systems, a blended system of fullerene and PVP was also investigated. PVP homopolymer and C<sub>60</sub> were solubilized in water; here, PVP with a molecular weight of 10,000 was used. **Figure 8** shows time-correlation function obtained at 90° and the  $q^2$ - $\Gamma$  plot. The time correlation data were fitted using a single exponential equation, and the hydrodynamic diameters were estimated to be ca. 230 nm. The diameter obtained here was much larger than those obtained from the PVP-C<sub>60</sub> micelle system, on the order of several tens of nanometers, which indicates that a mixed system does not favor the formation of micelles.

In a further attempt to control the micelle size, we solubilized free C<sub>60</sub> molecules into the

PVP-C<sub>60</sub> micelle core. The simple preparation of a desired sized micelle was possible with this concept through the continuous addition of C<sub>60</sub> to any PVP-C<sub>60</sub> micelle solution. **Figure 9** shows the size variation of the micelles upon the addition of C<sub>60</sub>. The hydrodynamic size presented in **Figure 9** at each C<sub>60</sub>/PVP-C<sub>60</sub> ratio is the dominant one for the clarity. The amount of C<sub>60</sub> added is represented as the molar ratio of added C<sub>60</sub> to PVP in the lateral axis of **Figure 9**. The micelle size (hydrodynamic diameter) increased gradually up to ca. 40 nm at the beginning of the fullerene addition, which is followed by a significant jump to >200 nm. The assembly size change is also presented in Figure S9, in which the size distributions are shown. We can see the clear shift of the assembly size by the addition of C<sub>60</sub>.

Coincidentally, this two-size range is similar to the range obtained for the PVP-C<sub>60</sub> samples, as shown in **Figure 4** and **Table 1**. In the PVP-C<sub>60</sub> dispersions, a small number of aggregates with 200 nm size formed in addition to a large number of micelles with 15–33 nm size. **Figure 9** suggests that the size of PVP-C<sub>60</sub> assemblies in water is not continuous but limited to two ranges: 15–40 nm and >200 nm. This means that the stable morphology is limited to a range of hydrodynamic diameter values, and that PVP-C<sub>60</sub> assembles into this morphology. We did not obtain further structural information on the 200 nm size aggregate from the DLS data, but we considered that the cluster might possess a certain structure. This is because, in fullerene containing polymer system, organized assemblies much larger than micellar size have been reported [11, 14, 29, 30]. This kind of assembly is referred to as a large compound micelle (LCM) [31,32], which was also found in our previous study [14].

The drastic change is observed at almost the same  $C_{60}$ /PVP monomer molar ratio for the different length of grafted PVP although some error might be included. This suggests that one fullerene molecule is stabilized by a certain number of PVP unit, and ca.100 PVP unit would be a lower threshold for stabilizing a fullerene molecule.

**Figure 10** shows TEM images of PVP- $C_{60}$  assemblies below and above the critical ratio of added  $C_{60}$ /PVP monomer. Immediately upon addition of free  $C_{60}$ , micelles with diameters ca. 20 nm were observed. At 0.02 molar ratio of added  $C_{60}$  to PVP monomer, however, we observed large aggregates with diameters of about 200 nm, which agrees with the results, obtained using DLS. The two size ranges of assembly observed here coincide with the ones observed in aqueous solution as shown in **Table 1**. The assembly formed in the solution is therefore hypothesized to be discontinuous in regard to size and to a certain morphology. Unfortunately, the detailed morphology cannot be uncovered by TEM observation in this system.

In summary, PVP-grafted fullerene was synthesized, and micelles with a ca. 20 nm diameter were formed. The micelle size could be controlled by adding fullerene with diameter up to 40 nm; however, a large assembly of a 200 nm diameter forms at a critical value of the  $C_{60}$ /PVP monomer ratio. The critical value of the  $C_{60}$ /PVP monomer ratio between different systems was found to be comparable regardless of the molecular weight of the PVP within the studied range. The PVP- $C_{60}$  micelle size can, therefore, be controlled by adjusting the  $C_{60}$ /PVP monomer ratio and by changing the amount of

solubilized fullerene. This size-tuning process may contribute to the practical application of PVP-C<sub>60</sub> to an *in vivo* system.

## **Conclusions**

The micelle formation of PVP-grafted fullerene and the effect of dissolving C<sub>60</sub> into the core of PVP-grafted fullerene micelles were investigated. Micelles formed in water were confirmed to be monodisperse, with diameters that could be controllable within 15–33 nm via the molecular weight of grafted PVP. Similar behavior for the PVP-C<sub>70</sub> system was observed. The solubilization of fullerene molecules into the core of the micelles was also demonstrated. Upon increase of the amount of added fullerene, the micelle diameter increased gradually and subsequently drastically increased to ca. 200 nm. The assembly formed in the solution is therefore hypothesized to be discontinuous in terms of size and limited to a certain morphology.

## **Acknowledgments**

We are greatly thankful to Prof. Kohji Yoshinaga (Professor Emeritus of Kyushu Institute of Technology) for his advice on the experiments, especially for the synthesis of the samples. We express our appreciation to Prof. Masato Yamamura (Kyushu Institute of Technology) for the help with the surface tension measurements. We also thank Dr. Tsuyoshi Takakura (mitsubishi Chemical) for valuable

comments regarding fullerenes. We are sincerely grateful to Dr. Suguru Motokucho (Nagasaki Univ.) and Mr. Noboru Wakayama (Kyushu Institute of Technology) for helping us with the GPC data treatment, and TEM observation. This work was financially supported by a grant-in-aid from Japan Society for the Promotion of Science (nos. 19750099 and 24850015).

### References

- (1) Prato M (1997) [60]Fullerene chemistry for materials science applications. *J Mater Chem* 7:1097 -1109
- (2) Giacalone F, Martin N (2006) Fullerene polymers: synthesis and properties. *Chem Rev* 106:5136 - 5190
- (3) Friedman SH, DeCamp DL, Sijbesma RP, Srdanov G, Wudl F, Kenyon GL (1993) Inhibition of the HIV-1 protease by fullerene derivatives: model building studies and experimental verification. *J Am Chem Soc* 115:6506 -6509
- (4) Gharbi N, Pressac M, Hadchouel M, Szwarc H, Wilson SR, Moussa F (2005) [60]Fullerene is a powerful antioxidant in vivo with no acute or subacute toxicity. *Nano Lett.* 5:2578 -2585
- (5) Lyon DY, Brunet L, Hinkal GW, Wiesner MR, Alvarez PJJ (2008) Antibacterial activity of fullerene water suspensions (nC<sub>60</sub>) is not due to ROS-mediated damage. *Nano Lett* 8:1539 -1543
- (6) Constantin C, Neagu M, Ion RM (2010) Fullerene–porphyrin nanostructures in photodynamic therapy. *Nanomedicine* 5:307 -317
- (7) Mousavi S Z MD, Nafisi S, Maibach HI (2017) Fullerene nanoparticle in dermatological and

- cosmetic applications. *Nanomedicine* 13:1071 -1087
- (8) Richardson CF, Schuster DI, Wilson SR (2000) Synthesis and characterization of water-soluble amino fullerene derivatives. *Org Lett* 2:1011 -1014
- (9) Ravi P, Dai S, Wang C, Tam KC (2007) Fullerene containing polymers: A review on their synthesis and supramolecular behavior in solution. *J. Nanosci. Nanotechnol.* 7:1176 -1196
- (10) Kawauchi T, Kumaki J, Yashima E (2006) Nanosphere and nanonetwork formations of [60]fullerene-end-capped stereoregular poly(methyl methacrylate)s through stereocomplex formation combined with self-assembly of the fullerenes. *J Am Chem Soc* 128:10560 -10567
- (11) Tan C H, Ravi P, Dai S, Tam K C (2004) Solvent-induced large compound vesicle of [60]fullerene containing poly(tert-butyl methacrylate). *Langmuir* 20:9901 -9904
- (12) Ravi P, Dai S, Tan C H, Tam K C (2005) Self-assembly of alkali-soluble [60]fullerene containing poly(methacrylic acid) in aqueous solution. *Macromolecules* 38: 993-939
- (13) Zhou G, Harruna I I, Zhou W L, Aicher W K, Geckeler K E (2007) Nanostructured thermosensitive polymers with radical scavenging ability. *Chem Euro J* 13: 569-573
- (14) Mouri E, Moriyama M (2017) Fabrication of structure-preserving monodisperse particles of PMMA-grafted fullerenes. *Fibers and Polymers* 18: 2261-2268
- (15) Dai S, Ravi P, Tan CH, Tam KC (2004) Self-assembly behavior of a stimuli-responsive water-soluble [60]fullerene-containing polymer. *Langmuir* 20: 8569-8575

- (16) Okamura H, Terauchi T, Minoda M, Fukuda T, Komatsu K (1997) Synthesis of 1,4-dipolystyryldihydro [60]fullerenes by using 2,2,6,6-tetramethyl-1-piperidinoxypiperidine as a radical source. *Macromolecules* 30: 5279-5284
- (17) Okamura H, Ide N, Minoda M, Komatsu K, Fukuda T (1998) Solubility and micellization behavior of C<sub>60</sub> Fullerenes with two well-defined polymer arms. *Macromolecules* 31: 1859-1865
- (18) Khairullin II, Chen Y-H, Hwang L-P, (1997) Evidence for electron charge transfer in the polyvinylpyrrolidone-C<sub>60</sub> system as seen from ESR spectra. *Chem Phys Lett* 275: 1-6
- (19) Sushko ML, Tenhu H, Klenin SI (2002) Static and dynamic light scattering study of strong intermolecular interactions in aqueous solutions of PVP/C<sub>60</sub> complexes. *Polymer* 43: 2769-2775
- (20) Török G, Lebedev VT, Cser L, Orlova DN, Sibilev AI, Zgonnik VN, Melenevskaya EY, Vinogradova LV, Sibileva MA (2004) Dynamics of complexes of poly(*N*-vinylpyrrolidone)-C<sub>60</sub> in aqueous solution. *Physica B* 350: e415 - e418
- (21) Tarassova E, Aseyev V, Filippov A, Tenhu H (2007) Structure of poly(vinyl pyrrolidone)-C<sub>70</sub> complexes in aqueous solutions. *Polymer* 48: 4503-4510
- (22) Souto GD, Pohlmann AR, Guterres SS (2015) Ultraviolet A irradiation increases the permeation of fullerenes into human and porcine skin from C<sub>60</sub>-Poly(vinylpyrrolidone) aggregate dispersions. *Skin Pharma-col Physiol* 28: 22-30
- (23) Oriana S, Aroua S, Söllner J O B, Ma X-J, Iwamoto Y, Yamakoshi Y (2013) Water-soluble C<sub>60</sub>- and

- C<sub>70</sub>-PVP polymers for biomaterials with efficient <sup>1</sup>O<sub>2</sub> generation. Chem Commun 49:9302 -9304
- (24) Aroua S, Tiu EGV, Ayer M, Ishikawa T, Yamakoshi Y (2015) RAFT synthesis of poly(vinylpyrrolidone) amine and preparation of a water-soluble C<sub>60</sub>-PVP conjugate. Polym Chem 6: 2616 -2619
- (25) Yamada S, Wang Z, Mouri E, Yoshinaga K (2009) Crystallization of titania ultra-fine particles from peroxotitanic acid in aqueous solution in the presence of polymer and incorporation into poly(methyl methacrylate) via dispersion in organic solvent. Colloid Polym Sci 287:139 -146
- (26) Noskov BA, Akentiev AV, Miller R (2002) Dynamic surface properties of poly(vinylpyrrolidone) solutions. J Coll Int Sci 255:417 -424
- (27) Brandrup J, Immergut E H, Grulke E A, Abe A, Bloch D R Eds. (1999) Polymer Handbook John Wiley & Sons, New Jersey
- (28) Mouri E, Moroi S *Submitted*.
- (29) Tan CH, Ravi P, Dai S, Tam KC, Gan LH, (2004) Solvent-induced large compound vesicle of [60]fullerene containing poly(tert-butylmethacrylate). Langmuir 20:9882 -9884
- (30) Ravi P, Dai S, Hong KM, Tam KC, Gan LH (2005) Self-assembly of C<sub>60</sub> containing poly(methyl methacrylate) in ethyl acetate/decalin mixtures solvent. Polymer 46:4714-4721
- (31) Zhang L, Eisenberg A (1996) Multiple morphologies and characteristics of “crew-cut” micelle-like aggregates of polystyrene-*b*-poly(acrylic acid) diblock copolymers in aqueous solutions. J Am Chem

Soc 118:3168 -3181

(32)Moffitt M, Vali H, Eisenberg A (1998) Spherical assemblies of semiconductor nanoparticles in water-soluble block copolymer aggregates. Chem Mater 10:1021 -1028

## Figure Captions

**Figure 1.** UV–vis spectra for PVP and PVP- $C_{60}$  aqueous solutions.

**Figure 2.** Surface tension measurements for the PVP10k- $C_{60}$  aqueous solution.

**Figure 3.** Time correlation function for the PVP- $C_{60}$  aqueous solutions at a scattering angle of  $90^\circ$ : (a) PVP3k- $C_{60}$ , (b) PVP10k- $C_{60}$ , (c) PVP30k- $C_{60}$ , and (d) PVP45k- $C_{60}$ .

**Figure 4.** Plots of  $\Gamma$  vs.  $q^2$  for the PVP- $C_{60}$  aqueous solutions; the diffusion coefficient was evaluated from the slope of the plot: (a) PVP3k- $C_{60}$ , (b) PVP10k- $C_{60}$ , (c) PVP30k- $C_{60}$ , and (d) PVP45k- $C_{60}$ .

**Figure 5.** TEM images of assemblies formed in aqueous solution of (a) PVP3k- $C_{60}$  and (b) PVP10k- $C_{60}$ .

**Figure 6.** Effect of the molecular weight of PVP on the micelle size for the PVP- $C_{60}$  and PVP- $C_{70}$  systems.

**Figure 7.**  $\Gamma$  vs.  $q^2$  plot for PVP10k- $C_{60}$  in (a) a 0.15 M NaCl aqueous solution and (b) an ethanol solution.

**Figure 8.** DLS data for the PVP/ $C_{60}$  mixed system. (a) Time-correlation function at a scattering angle of  $90^\circ$  and (b)  $\Gamma$  vs.  $q^2$  plot.

**Figure 9.** Change in hydrodynamic diameter upon addition of free  $C_{60}$  plotted against (a) the ratio of added  $C_{60}$  to PVP- $C_{60}$  and (b) the molar ratio of added  $C_{60}$  to PVP monomer.

**Figure 10.** TEM images of PVP10k- $C_{60}$  in the process of fullerene solubilization at (a) 0.0061 and (b) 0.015 molar ratios of added  $C_{60}$  to PVP monomer.

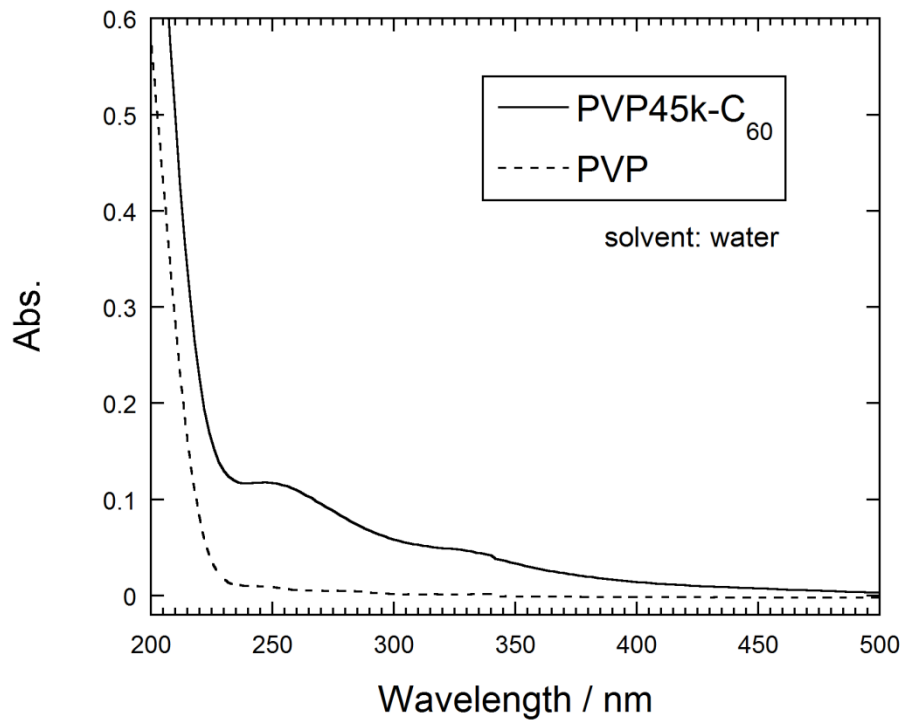


Fig.1

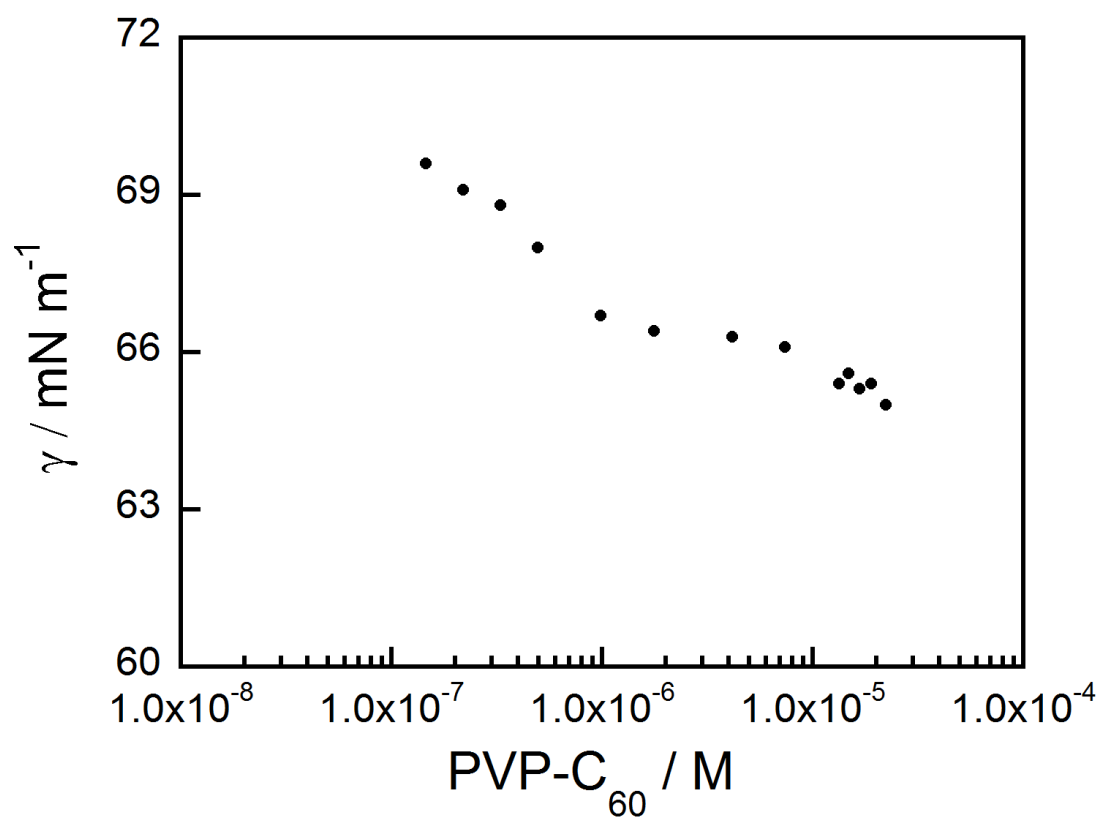


Fig.2

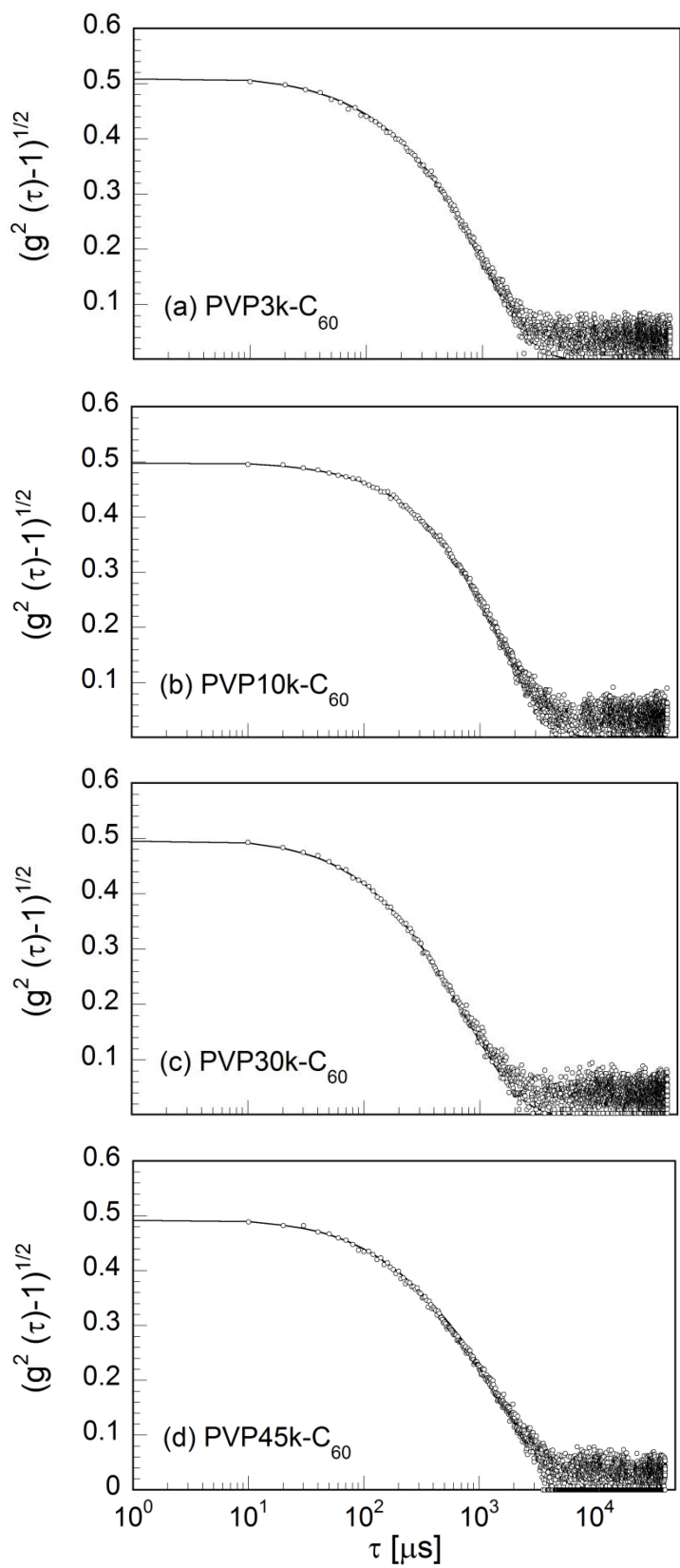


Fig.3

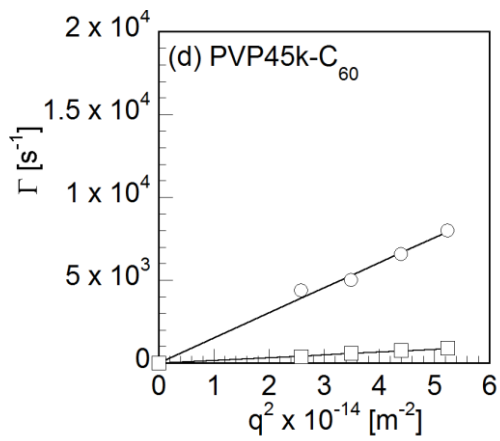
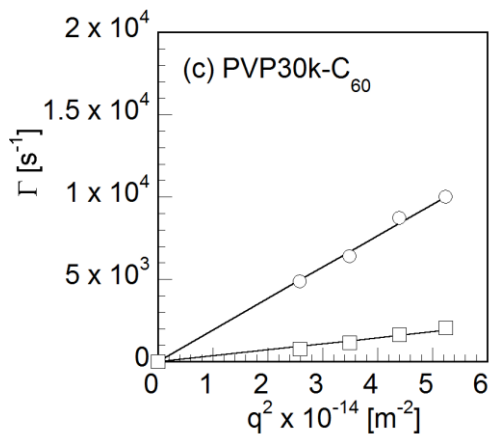
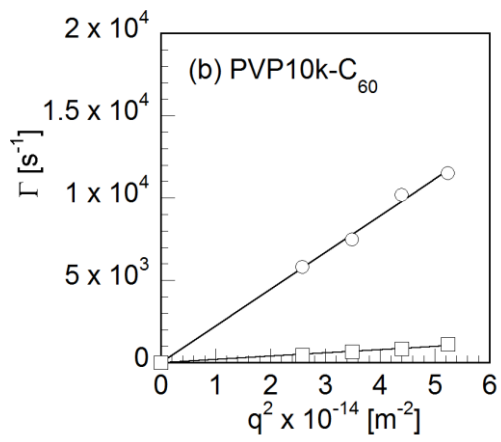
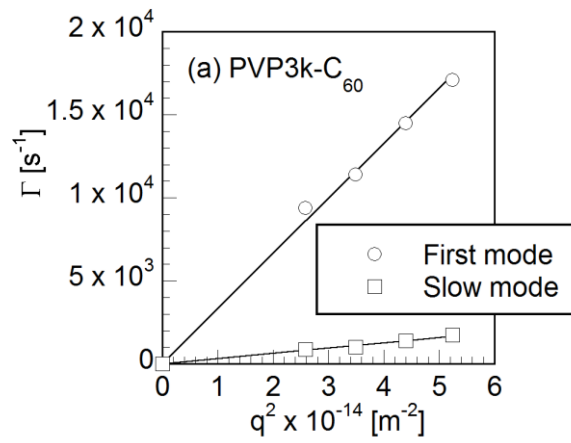


Fig.4

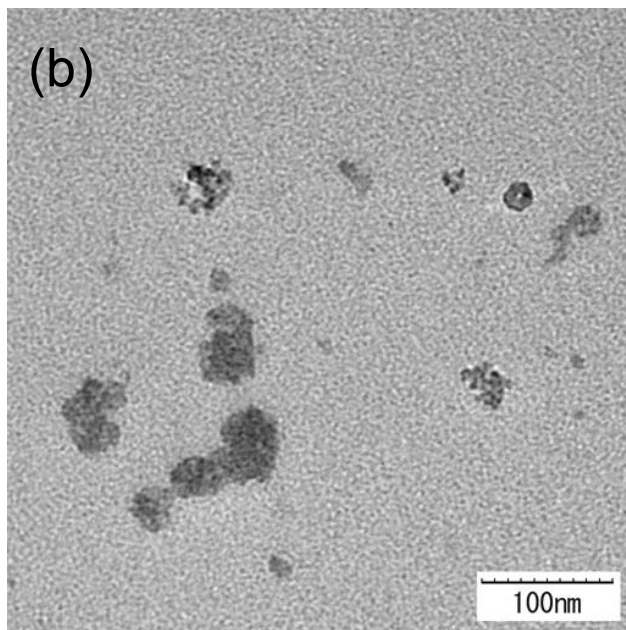
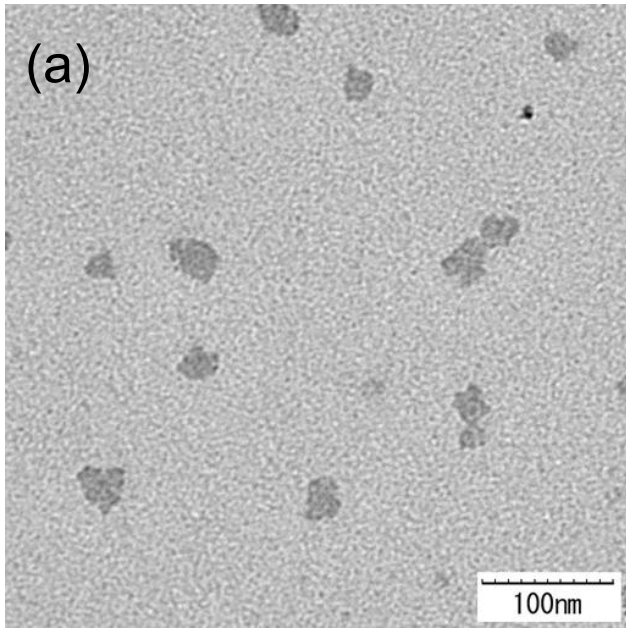


Fig.5

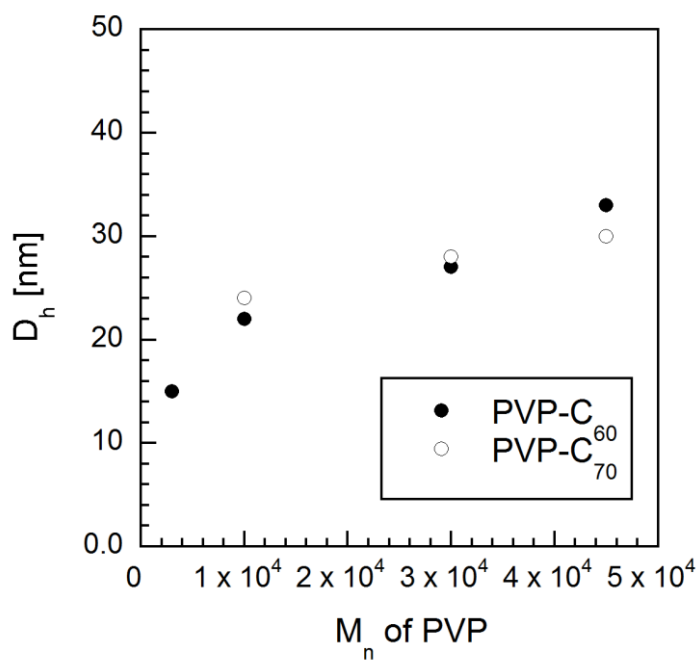


Fig. 6

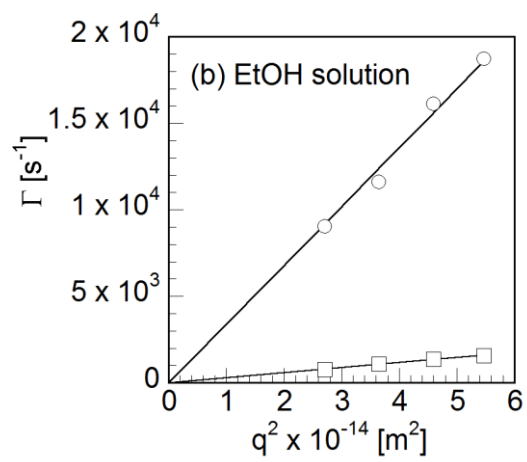
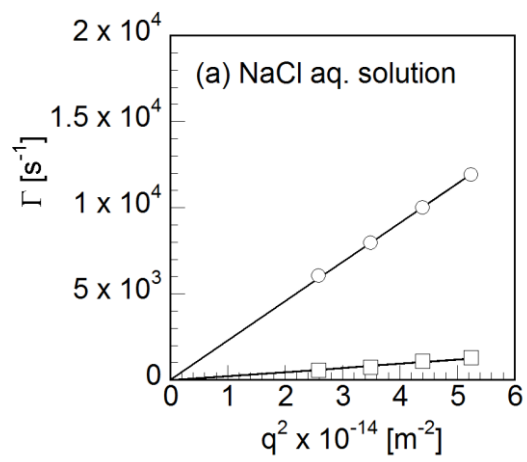


Fig. 7

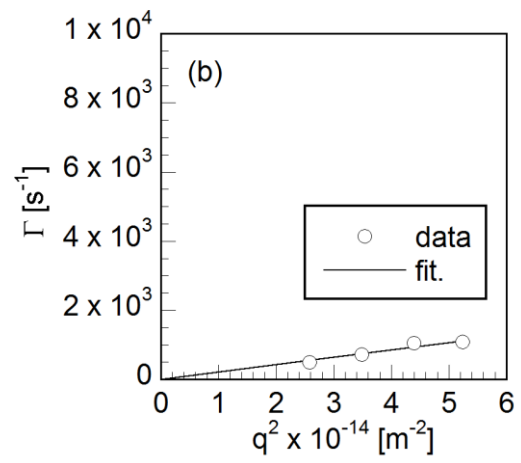
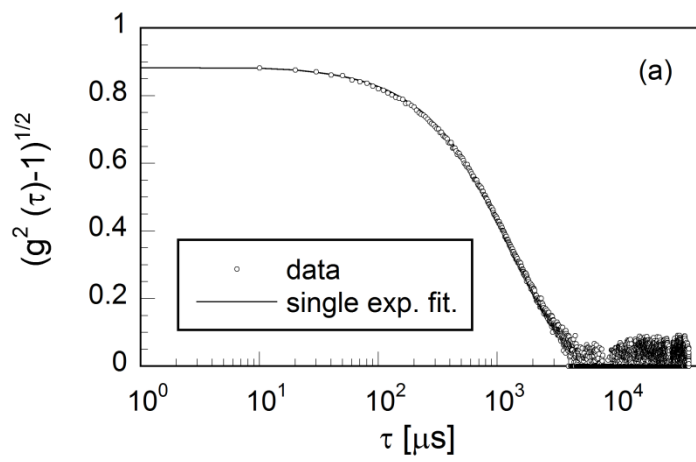


Fig. 8

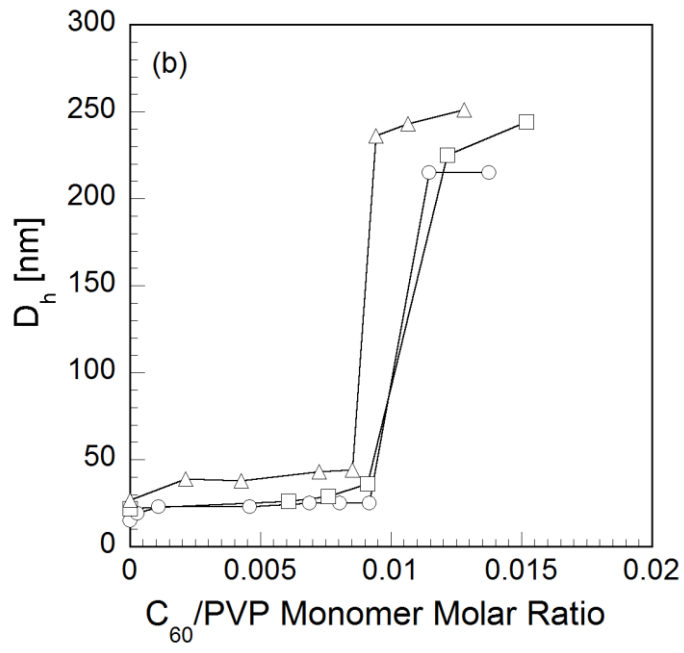
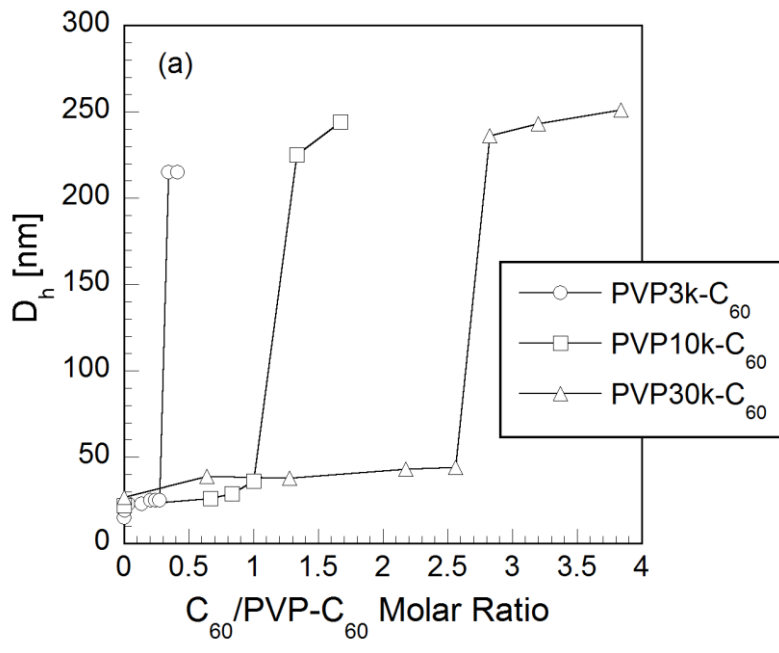
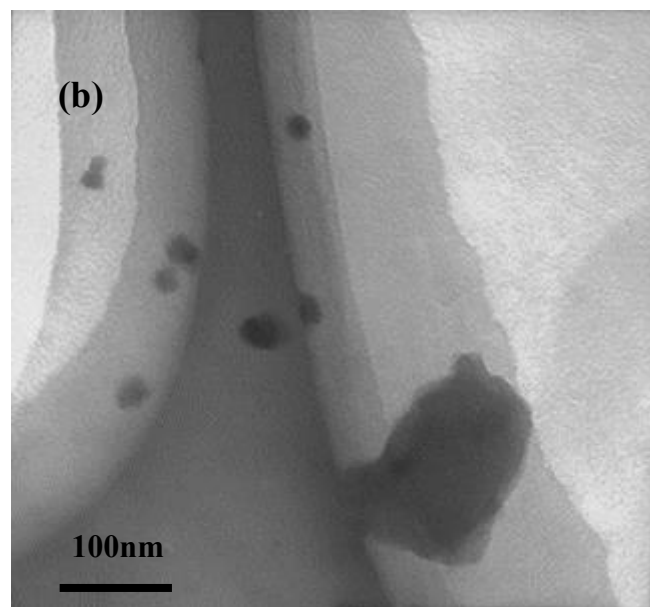
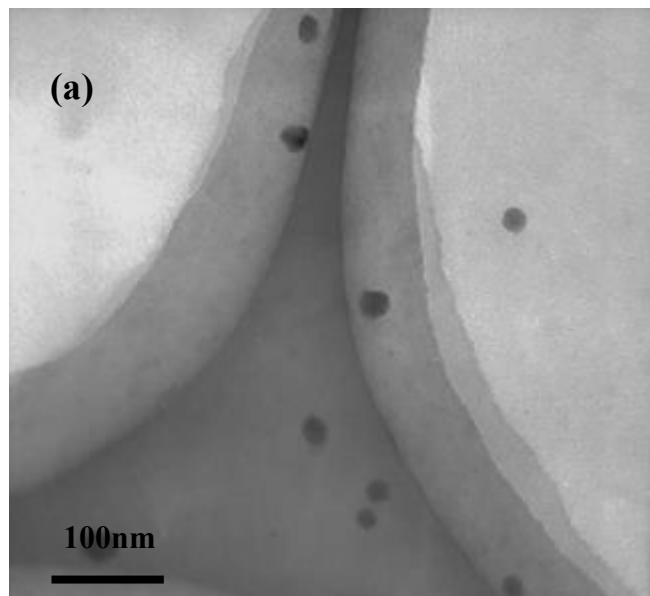


Fig. 9

Fig. 10



**Table 1.** Characteristics of PVP-C<sub>60</sub> and PVP-C<sub>60</sub> assembly size in aqueous solution.

Sample Code	M <sub>n</sub> <sup>*</sup>	M <sub>n</sub> <sup>**</sup> (PEG)	M <sub>n</sub> <sup>**</sup> (PSt)	M <sub>w</sub> /M <sub>n</sub> <sup>**</sup> (PSt)	D <sub>h</sub> / nm <sup>§</sup> (Number fraction, %)
PVP3k-C <sub>60</sub>	3,000	1,400	5,000	1.19	15 (ca. 100), 154 (~ 0)
PVP10k-C <sub>60</sub>	10,000	4,300	13,000	1.16	22 (99.69), 246 (0.31)
PVP30k-C <sub>60</sub>	30,000	10,000	25,000	1.29	26 (99.82), 136 (0.18)
PVP45k-C <sub>60</sub>	-	23,000	45,000	1.56	33 (99.84), 289 (0.16)

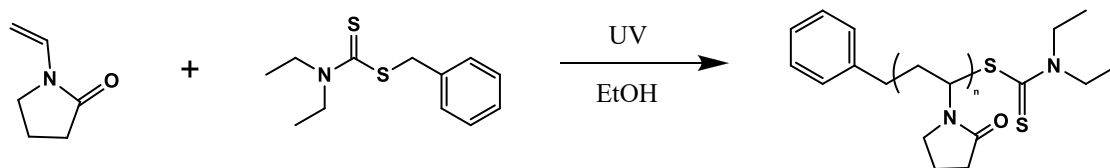
\*PVP homopolymer molecular weight estimated by <sup>1</sup>H-NMR measurement.

\*\*PVP homopolymer molecular weight estimated by GPC measurement with PEG and PSt standards.

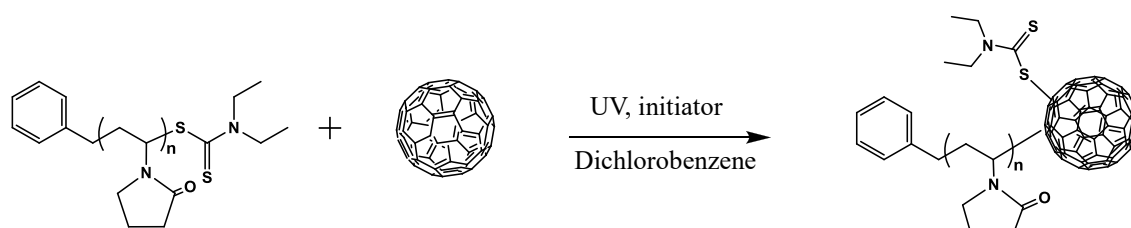
§Estimated by DLS measurement. Number fractions are from Maquardt method analysis.

**Table 2.** Characteristics of PVP10k-C<sub>60</sub> assembly.

Solvent	D <sub>h</sub> / nm (Number fraction, %)
ethanol	12 (ca. 100), 132 (~ 0)
0.15 M NaCl aq.	20 (99.93), 206 (0.07)
Water (added C <sub>60</sub> )	231 (100)



**Scheme 1.** Polymerization of PVP.



**Scheme 2.** Reaction between PVP and fullerene C<sub>60</sub>.

Association Behaviours of  
Poly(*N*-vinyl pyrrolidone)-*grafted* Fullerenes in Aqueous  
Solution

Supporting Information

Emiko Mouri\*, Sanami Moroi,

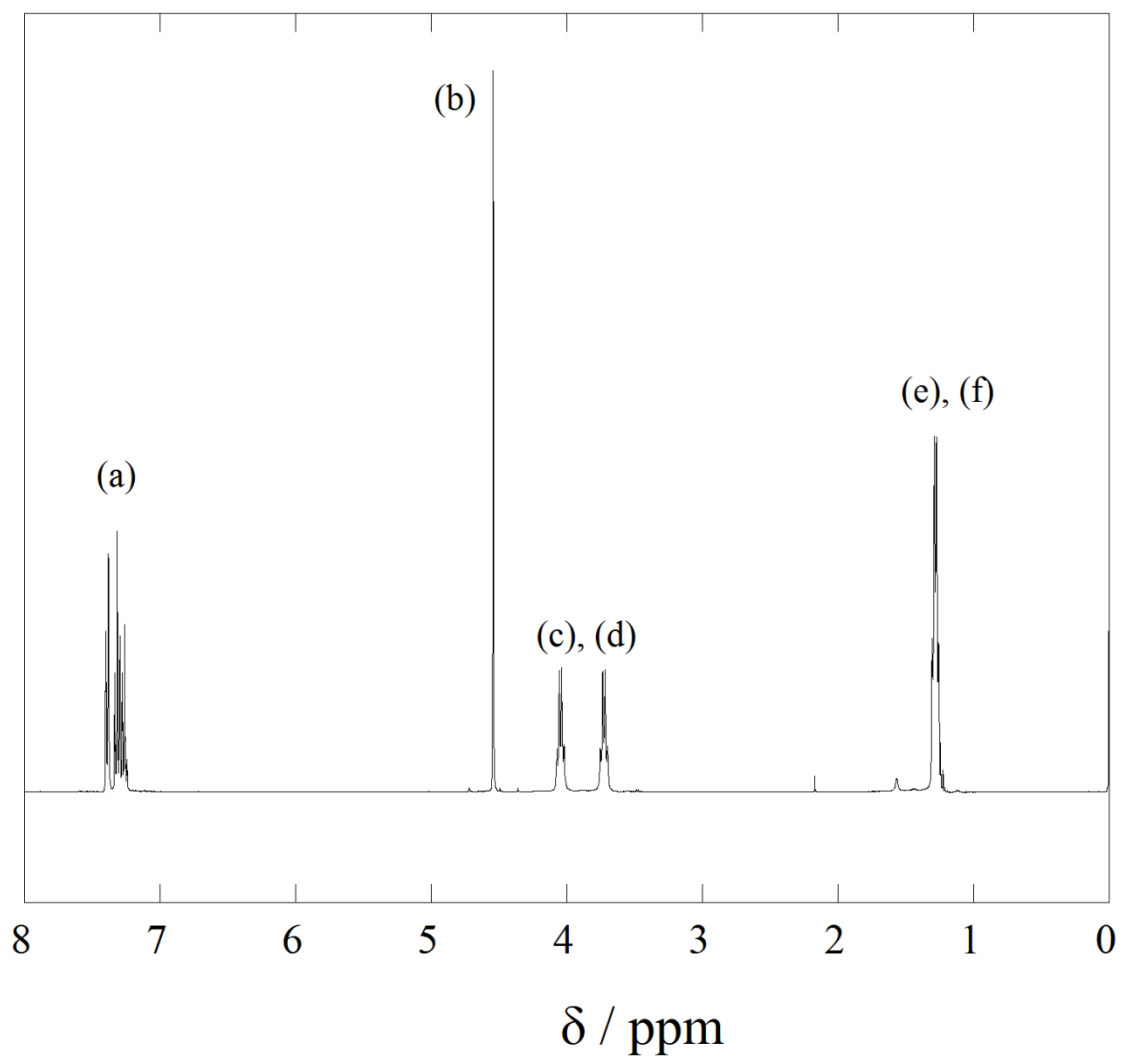
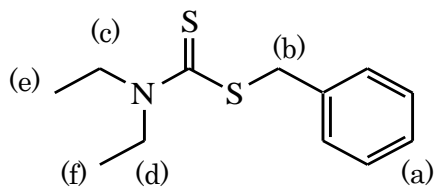


Figure S1. <sup>1</sup>H-NMR spectrum of benzyl *N,N*-dithiocarbamate (BDDC).

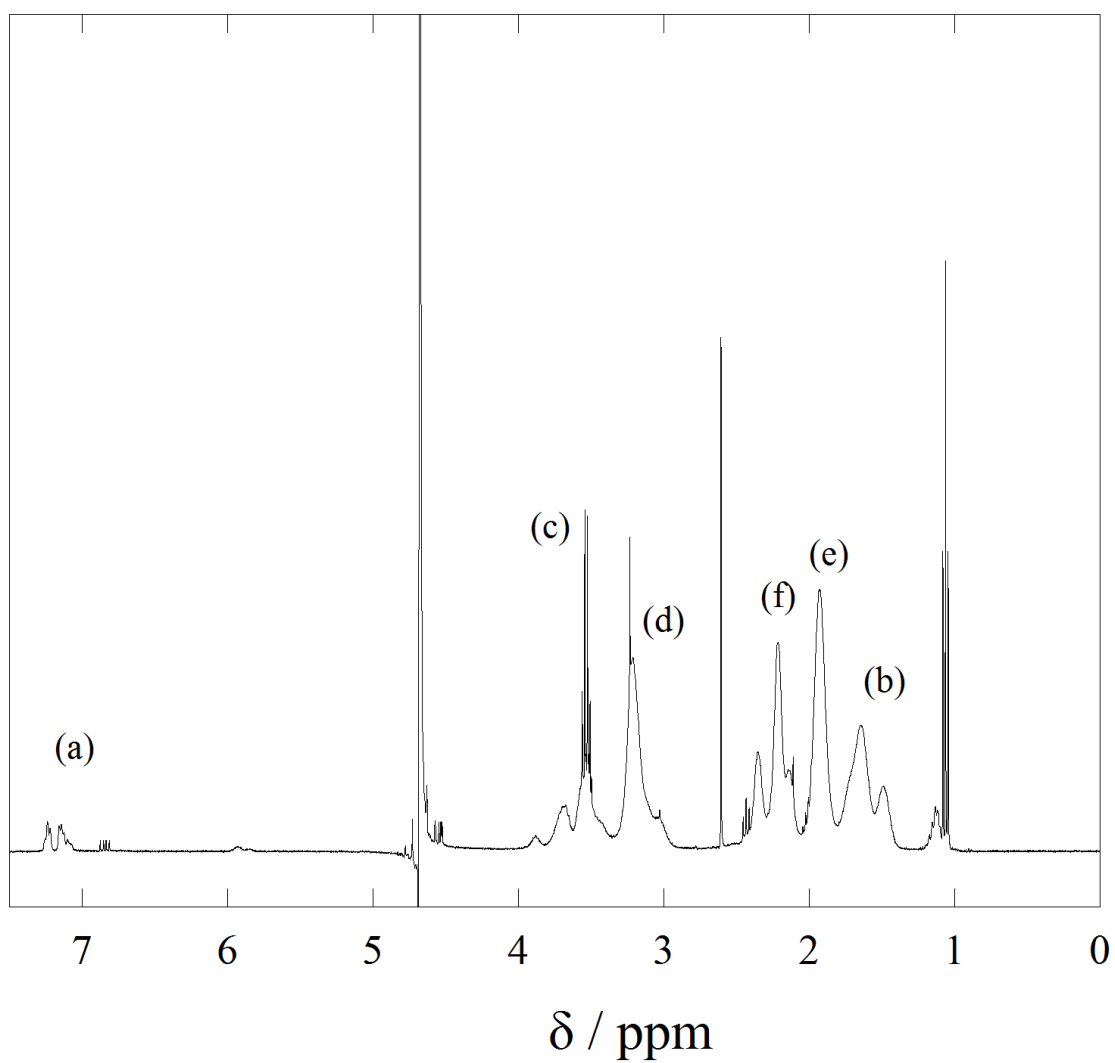
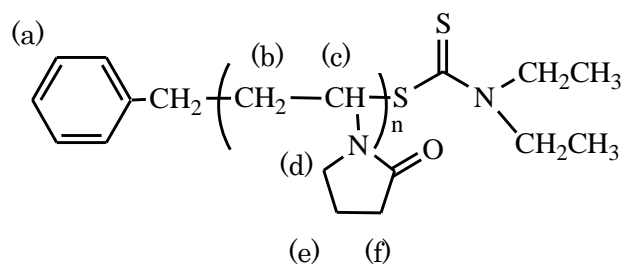


Figure S2.  $^1\text{H-NMR}$  spectrum of PVP.

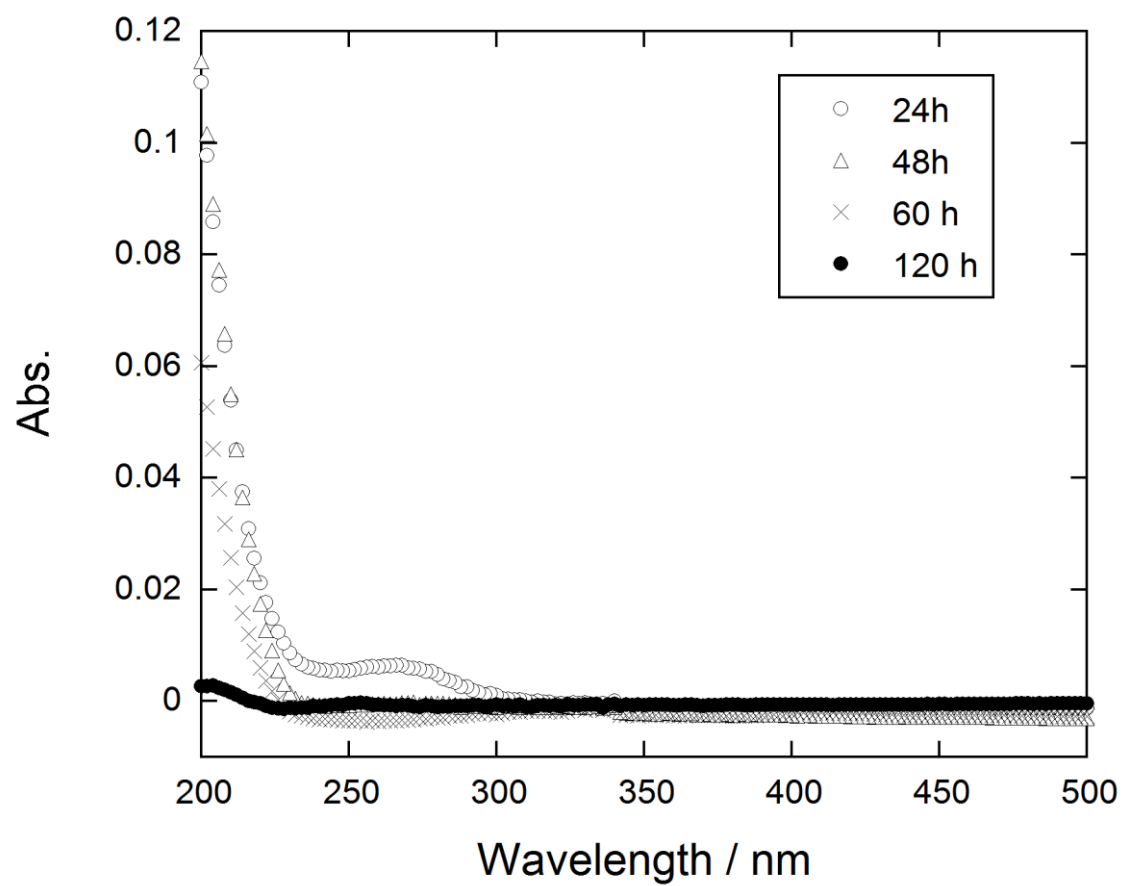


Figure S3. UV-vis spectrum change of dialyzing out-side water during the dialysis of PVP-C<sub>60</sub>.

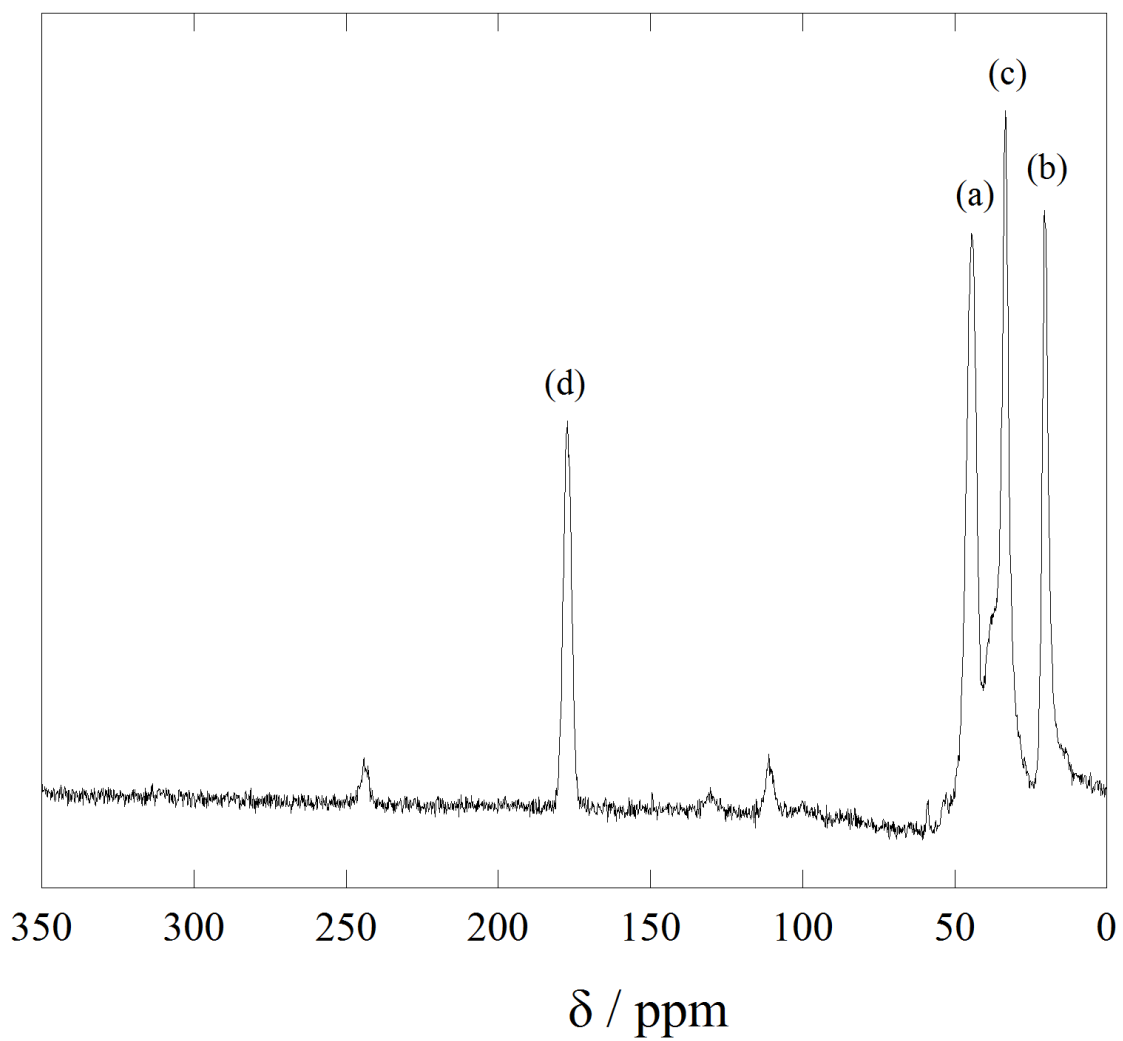
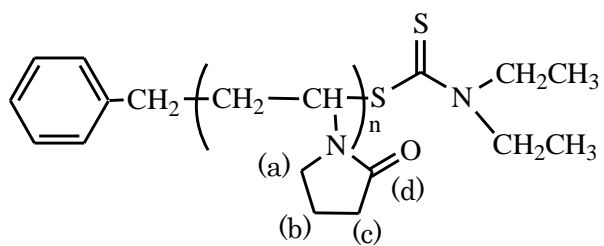


Figure S4.  $^{13}\text{C}$ -NMR spectrum of PVP.

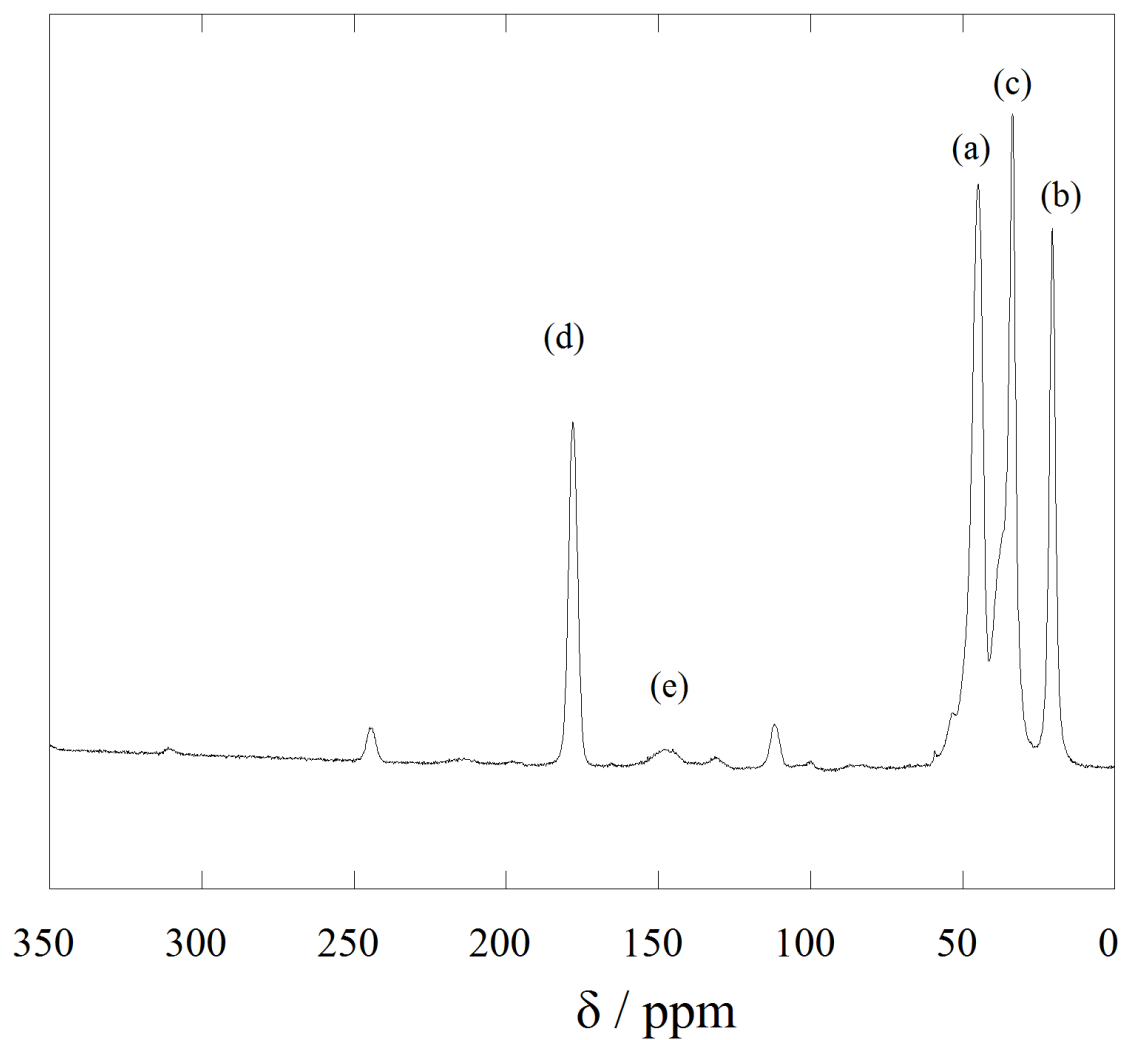
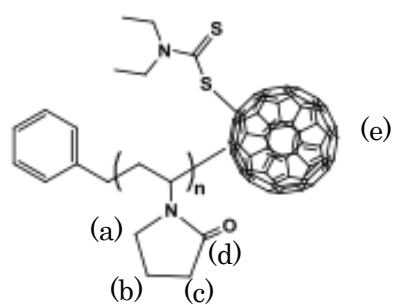


Figure S5. <sup>13</sup>C-NMR spectrum of PVP-C<sub>60</sub>

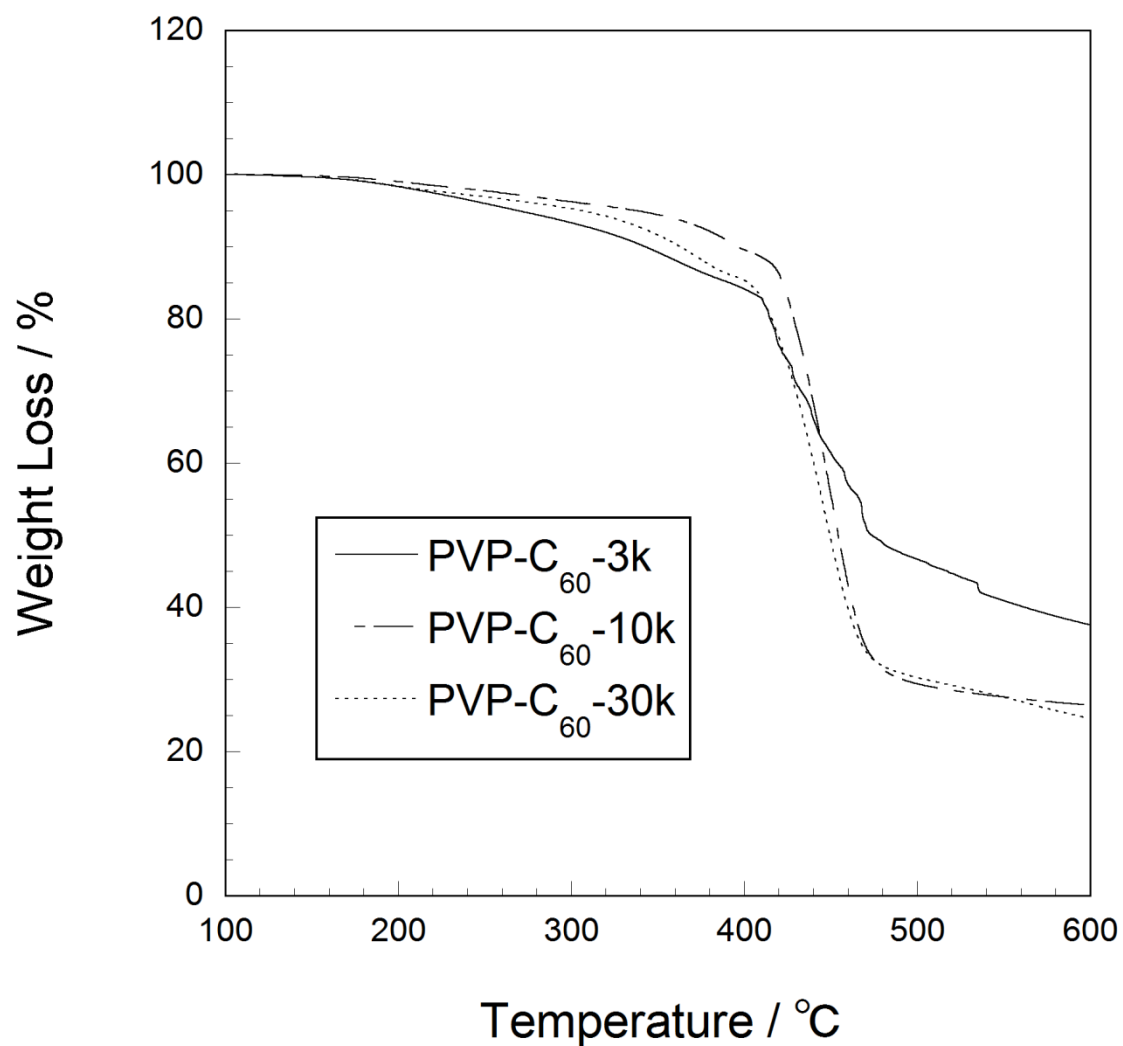


Figure S6. TGA curves of PVP-C<sub>60</sub>. In principle, the residue at 600 C should be different between 10k and 30k, however, the residue of the two sample is similar. The polydispersity of PVP would contribute the result.

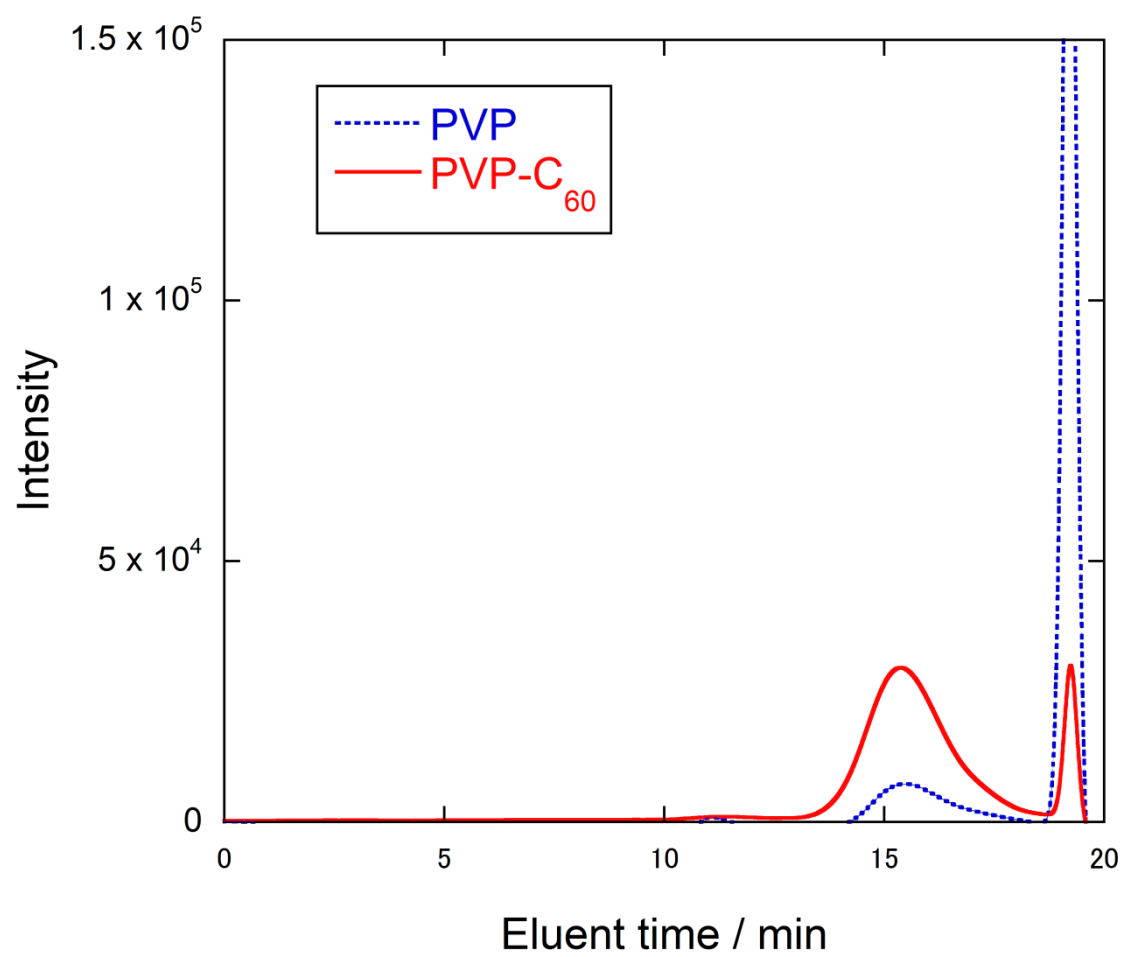


Figure S7. GPC curves for PVP and PVP-C<sub>60</sub>.

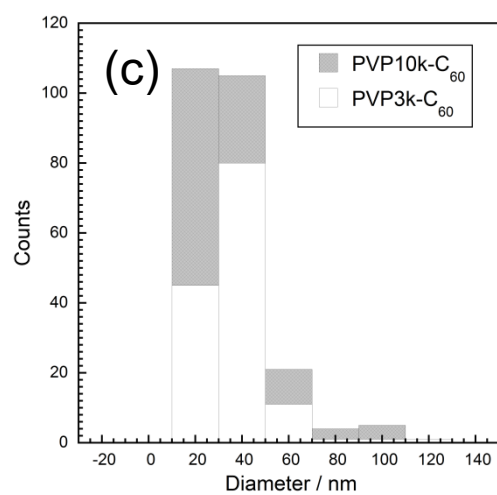
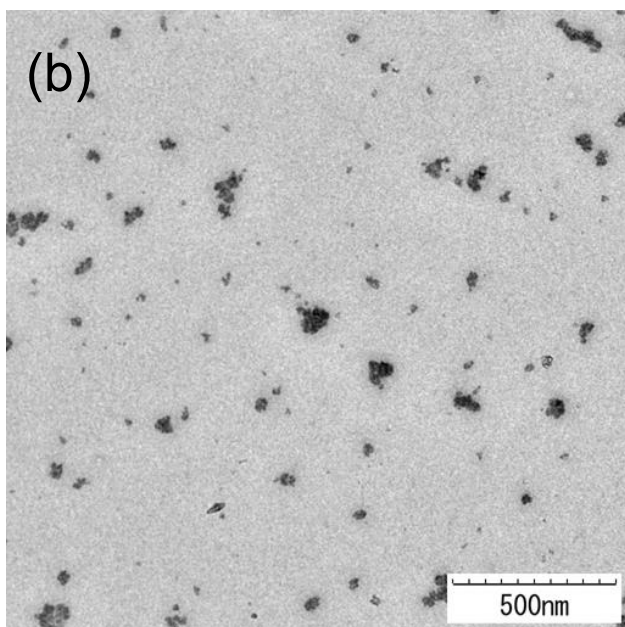
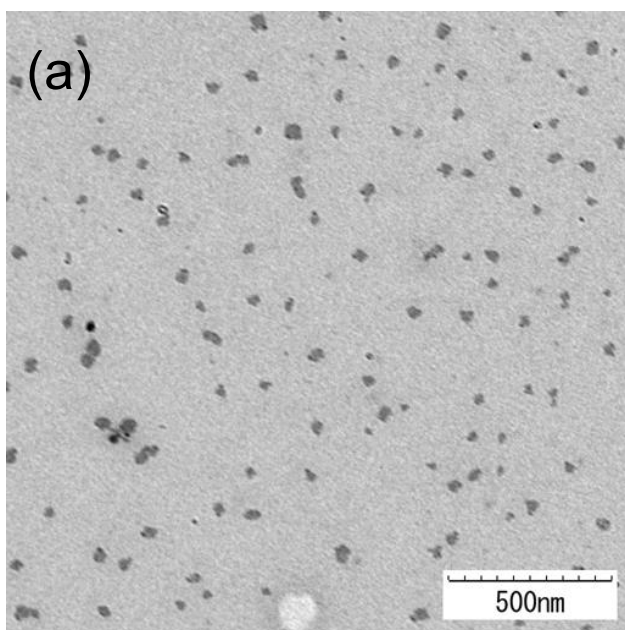


Figure S8. TEM images of (a) PVP3k-C<sub>60</sub> and (b) PVP10k-C<sub>60</sub>. Distribution of diameter is presented in

(c).

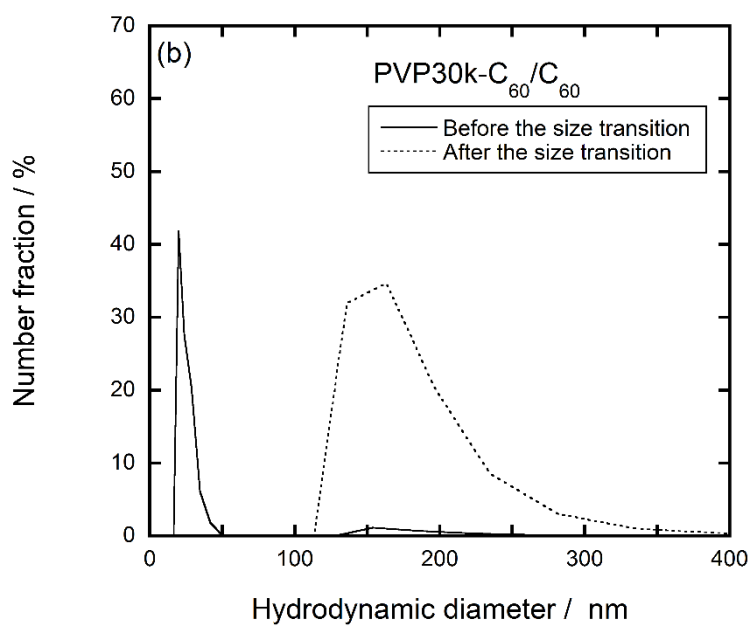
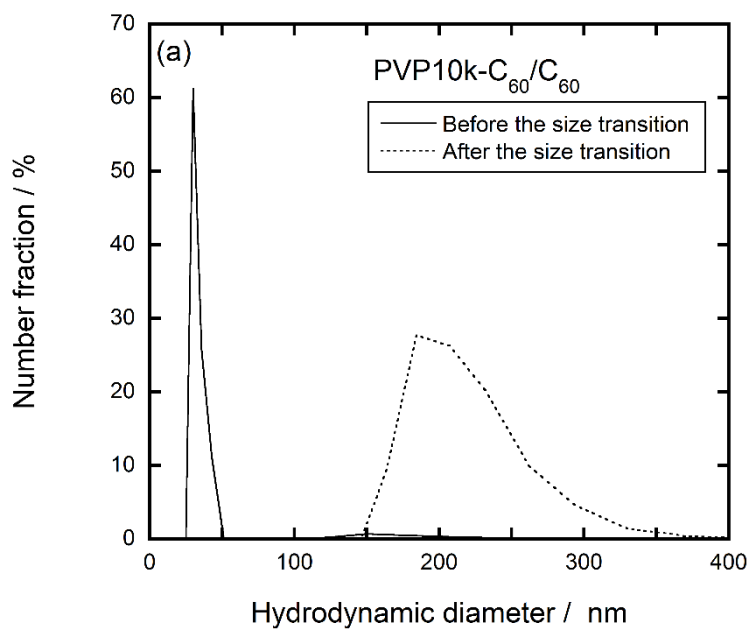


Figure S9. Number-based fraction analyzed by by Marquardt method for PVP-C<sub>60</sub>/C<sub>60</sub> systems before and after the size transition: (a) PVP10k-C<sub>60</sub>/C<sub>60</sub> and (b) PVP30k-C<sub>60</sub>/C<sub>60</sub>.

Table S1. Feeds, irradiation conditions, and yields in PVP polymerization.

Sample code	<i>N</i> -vinyl pyrrolidone/ ml	BDDC / mg	Ethanol / ml	Irradiation time / h	Yields / %
PVP3k	5	332	2	4	40
PVP10k	3	45.0	3	5	68
PVP30k	3	16.9	3	5	30
PVP45k	6	33.7	1.5	5	60

Table S2. Feeds and irradiation conditions in PVP-C<sub>60</sub> preparation.

Sample code	PVP / mg	C <sub>60</sub> / mg	1-hydroxy-cyclohexylphenyl ketone /mg	dichlorobenzene / ml	Irradiation time / h
PVP3k-C <sub>60</sub>	60	43	4.1	6	8
PVP10k-C <sub>60</sub>	60	13	1.2	6	8
PVP30k-C <sub>60</sub>	60	4	0.4	6	12
PVP45k-C <sub>60</sub>	60	3	0.3	6	12

Table S3. Characteristics of PVP-C<sub>60</sub> and PVP-C<sub>60</sub> assembly size in aqueous solution.

Sample Code	M <sub>n</sub> <sup>*</sup>	M <sub>n</sub> <sup>**</sup> (PEG)	PVP:C <sub>60</sub> <sup>§</sup>
PVP3k-C <sub>60</sub>	3,000	1,400	1 : 1.2
PVP10k-C <sub>60</sub>	10,000	4,300	1 : 2.1
PVP30k-C <sub>60</sub>	30,000	10,000	1 : 4.5

\*Estimated by <sup>1</sup>H-NMR measurement.

\*\*Estimated by GPC measurement with PEG standards.

§Calculated from TGA data and number-averaged molecular weights obtained by GPC with PEG standards.

Table S4. Number-based analysis result from DLS data analysis.

Sample code	D <sub>1</sub>	Standard deviation	D <sub>2</sub>	Standard deviation
PVP3k-C <sub>60</sub>	9.6	±1.7	101.7	±24.9
PVP10k-C <sub>60</sub>	24.0	±2.7	161.3	±37.7
PVP30k-C <sub>60</sub>	24.9	±5.3	-	-
PVP45k-C <sub>60</sub>	32.7	±5.8	204.9	±44.9

Analysis based on data obtained at the scattering angle of 90° by Marquardt method.

Table S5. Number-based analysis result from DLS data analysis.

Sample condition	D <sub>1</sub>	Standard deviation	D <sub>2</sub>	Standard deviation
PVP10k-C <sub>60</sub> /EtOH	10.8	±1.6	94.9	±21.9
PVP10k-C <sub>60</sub> /NaCl aq.	16.1	±2.0	137.7	±33.4
PVP10k /C <sub>60</sub>	-	-	169.7	±38.2

Analysis based on data obtained at the scattering angle of 90° by Marquardt method.

Table S6. Sample preparation conditions for C<sub>60</sub>-solubilization into micelles.

Sample code	PVP/gL <sup>-1</sup>	PVP/ml	C <sub>60</sub> /gL <sup>-1</sup>	C <sub>60</sub> /μl
PVP3k-C <sub>60</sub>	0.6	2	0.01	192-9600
PVP10k-C <sub>60</sub>	0.8	2	0.01	6-600
PVP30k-C <sub>60</sub>	0.8	2	0.01	2-11